ORIGINAL ARTICLE



Sagittal Imbalance May Lead to Higher Risks of Vertebral Compression Fractures and Disc Degeneration—A Finite Element Analysis

Koji Matsumoto^{1,2}, Anoli Shah¹, Amey Kelkar¹, Muzammil Mumtaz¹, Yogesh Kumaran¹, Vijay K. Goel¹

- BACKGROUND: Sagittal balance is an important clinical parameter of the spine for its normal function. Maintenance of the sagittal balance is crucial in the clinical management of spinal problems.
- METHODS: Three different finite element models with spinal alignments based on Schwab's classification were developed: (1) Balanced/Normal model (sagittal vertical axis [SVA] = 0 mm, lumbar lordosis [LL] = 50° , thoracic kyphosis [TK] = 25° , pelvic incidence [PI] = 45° , pelvic tilt [PT] = 10° , sacral slope [SS] = 35°); (2) Balanced with compensatory mechanisms/Flatback model (SVA = 50 mm, LL = 20° , TK = 20° , PI = 45° , PT = 30° , SS = 15°); and (3) Imbalanced/Hyperkyphotic model (SVA = 150 mm, LL = -5° , TK = 25° , PI = 45° , PT = 40° , SS = 5°). All 3 models were subjected to the follower loads simulating bodyweight/muscular contractions along with the moments to simulate flexion, extension, lateral bending, and axial rotation. The maximum cortical vertebral stress, annular stress, and intradiscal pressure (IDP) were calculated and compared.
- RESULTS: The results showed that the hyperkyphotic model had higher stresses in the vertebrae (25% higher), the annulus fibrosus (48% higher) and the IDP (8% higher) than the normal models in flexion. The segments near the thoracolumbar junction (T10-L1) showed the highest

increase in the vertebral body stress, the annulus fibrosus stress, and the IDP.

■ CONCLUSIONS: This study showed that the imbalance in sagittal alignment might be responsible for disc degeneration and atraumatic vertebral fractures at the thoracolumbar regions, supporting clinical findings.

INTRODUCTION

he sagittal balance of the spine is vital for its normal function. It is one of the essential clinical parameters for the management of spinal problems. Sagittal balance largely contributes to the quality of life (QOL) compared to the coronal balance. There are variations on the degree of normal curvature, but balanced spinal alignment allows optimal distribution of forces across the spinal column. The disruption of this equilibrium by pathologic processes, primarily aging, results in deformity. Adult spinal deformity (ASD) significantly impairs patients' QOL due to low back pain, gastroesophageal reflux disease, and deterioration of appearance, which are serious problems. Schwab et al. described the concept of using spinopelvic parameters such as sagittal vertical axis (SVA), lumbar lordosis (LL), thoracic kyphosis (TK), pelvic incidence (PI), pelvic tilt (PT), and sacral slope (SS) to classify ASD.

Key words

- Adult spinal deformity
- Finite element modeling
- Sagittal balance
- Schwab's classification

Abbreviations and Acronyms

3D: 3-dimensional

ASD: Adult spinal deformity
CT: computed tomography

DDD: degenerative disc disease **FE**: finite element

HK: Hyperkyphotic IDP: intradiscal pressure LL: lumbar lordosis

MRI: magnetic resonance imaging

PI: pelvic incidence PT: pelvic tilt QOL: quality of life ROM: range of motion SS: sacral slope SVA: sagittal vertical axis TK: thoracic kyphosis

From the ¹Engineering Center for Orthopedic Research Excellence (E-CORE), Departments of Bioengineering and Orthopaedic Surgery, University of Toledo, Toledo, Ohio, USA; and ²Department of Orthopaedic Surgery, Nihon University Itabashi Hospital, Tokyo, Japan

To whom correspondence should be addressed: Vijay K. Goel, Ph.D.

[E-mail: Vijay.Goel@utoledo.edu]

Citation: World Neurosurg. (2022) 167:e962-e971. https://doi.org/10.1016/j.wneu.2022.08.119

Journal homepage: www.journals.elsevier.com/world-neurosurgery

Available online: www.sciencedirect.com

1878-8750/\$ - see front matter © 2022 Elsevier Inc. All rights reserved.

increase in age, SVA, TK, and PT tend to increase while LL tends to decrease. These changes in the spinopelvic parameters lead to a rise in the incidence of spinal deformities in the aging population. To

Global sagittal imbalance consumes substantial energy and often results in painful compensatory mechanisms that can negatively influence a person's QOL. II Several parameters such as TK, LL, PI, and hip and leg positions can influence spinal alignment and thus sagittal balance. II During an imbalance, the compensation mechanism occurs by the muscle activation to keep spinal balance within normal limits. Further loss in spinal balance leads to the loss of LL, TK also reduces along with pelvis retroversion and flexion of knees to maintain sagittal balance. I2

Thus, it is important to understand the mechanics of imbalance and the limits of compensation mechanisms in certain patient populations. These clinical assessments help in understanding the progression of ASD. However, there are no biomechanical studies to understand the stresses on various components of the spine for 3 common sagittal alignments that a patient may experience through their lifetime.

The purpose of this study is to investigate the biomechanics of the relationship between the sagittal imbalance and its effect on the important biomechanical parameters such as intradiscal pressures, annulus stresses, and vertebral stresses. Thus, this study will aid in recognizing the areas potentially at risk to fractures or disc degeneration by studying the stresses as a function of sagittal curves.

METHODS

Development of the Finite Element Model

A nonlinear spine bony/ligamentous finite element model from Tr-femur was developed and validated (**Figure 1**). The model was developed from the computed tomography (CT) scans of a 55-year-old healthy adult male cadaveric spine without any abnormalities, deformities, tumors, or severe degeneration, based on radiographs. The 3-dimensional (3D) geometry was generated from r-mm slices of CT scans using MIMICS software (Materialise Inc., Leuven, Belgium). After the 3D reconstruction, the model was imported into Geomagic Studio software (Raindrop Geomagic Inc., Research Triangle Park, North Carolina, USA) to smoothen the surfaces to create patches and grids for meshing. The smoothened 3D geometry was meshed using the meshing software's IA-FE Mesh (University of Iowa, Iowa, USA) and Hypermesh (Altair Engineering, Inc., Troy, Michigan, USA).¹³

The vertebral bodies were modeled as a cortical bone shell of 0.5 mm thickness and the core of cancellous bone.¹³ The cortical

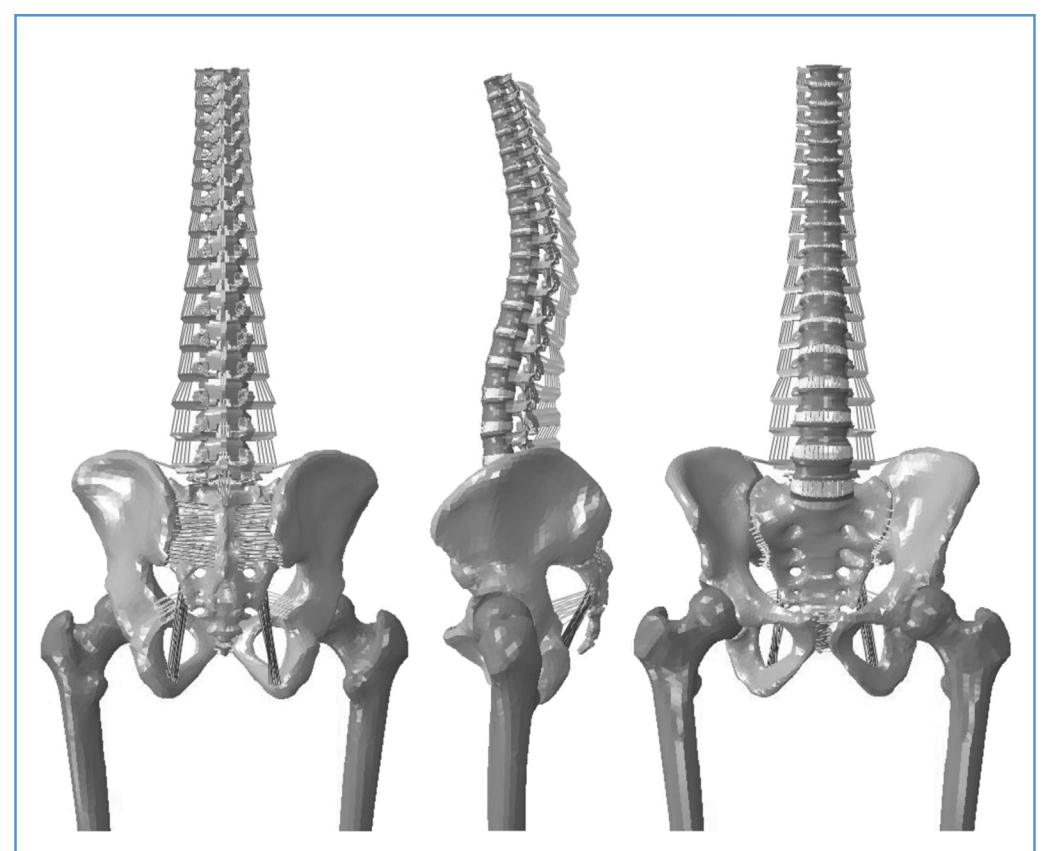


Figure 1. A nonlinear ligamentous validated finite element model with normal alignment from T1 to femur without rib cage.

Bony Structure	Type of Element	Modulus of Elasticity (MPa)	Poisson's Ratio
Cortical bone	Isotropic, elastic hexahedral elements	12000	0.3
Cancellous bone	Isotropic, elastic hexahedral elements	100	0.2
Intervertebral disc			
Thoracic segment-annulus fibrosus	Isotropic, elastic hexahedral elements	4.2	0.45
Thoracic segment-nucleus pulposus	Incompressible fluid, hexahedral elements	9	0.4999
Lumbar segment-annulus fibrosus	Neo Hookian, hexahedral elements	C10=0.348, D1=0.3	
Lumbar segment-nucleus pulposus	Incompressible fluid, hexahedral elements	1	0.4999
Annulus (fibers)	Rebar	357-550	0.3
Ligaments			
Anterior longitudinal	Tension-only, Truss elements	7.8(<12%), 20.0(>12%)	0.3
Posterior longitudinal	Tension-only, Truss elements	10.0(<11%), 20.0(>11%)	0.3
Ligamentum flavum	Tension-only, Truss elements	15.0(<6.2%), 19.5(>6.2%)	0.3
Intertransverse	Tension-only, Truss elements	10.0(<18%), 58.7(>18%)	0.3
Interspinous	Tension-only, Truss elements	10.0(<14%), 11.6(>14%)	0.3
Supraspinous	Tension-only, Truss elements	8.0(<20%), 15.0(>20%)	
Capsular	Tension-only, Truss elements	7.5(<25%), 32.9(>25%)	0.3
Joint			
Apophyseal joints	Non-linear soft contact, GAPPUNI elements	_	_

and cancellous bones were modeled as a linear elastic isotropic material. The thoracic kyphotic angle for this model was 25° and lumbar lordotic angle was 50° , representing normal spinal alignment as per Schwab classification. The intervertebral discs were composed of annulus and nucleus, the annulus was simulated as a composite solid with alternating $\pm 30^{\circ}$ collagen fibers modeled using REBAR elements with "no compression" property and nucleus was simulated as a linear elastic material. The facet joints were modeled using 3D gap elements with an initial defined clearance of 0.5 mm. All ligamentous structures were modeled as hypoelastic materials with "tension only" property. The material properties used for modeling the human thoracic-pelvis finite element (FE) model are listed in the Table 1. T

The model was validated using the range of motion (ROM) from in vitro studies. To the best of our knowledge, there is a lack of in vitro studies in the published literature with ROM data from T1 to S1 segments. Therefore, the validation study was carried out separately on the thoracic and lumbar segments of the FE model and with the data compared against literature data. The normal aligned spine model (SVA = 0 mm, LL = 50° , TK = 25° , PI = 45° , PT = 10° , SS = 35°) was validated.

Thoracic FE Model Validation

The thoracic spine from TI-TI2 was validated by comparing the motion behavior of the finite element model with the in vitro ROM

data from Watkins et al.¹⁷ Watkins et al. dissected the human cadaveric spine specimens from T1-T12; potted the T12 vertebra and applied a 2 Nm moment at T1 to simulate flexion, extension, and lateral bending. A 5 Nm moment was applied at T1 with 100 N of follower load for simulating the axial rotations in their in vitro study.¹⁷ This technique simulates the compressive forces on the spine in vivo and was applied onto the FE model by connecting adjacent vertebral bodies by utilizing the wire feature in ABAQUS (Dassault Systèmes, Vélizy-Villacoublay, France) and applying an axial-compressive load on the connector feature, bilaterally (Table 2). The same loading scenarios were simulated on the FE model from T1-T12 for validation of the model. T12 was fixed and the loads were applied at T1. The ROM of T1-T12 was evaluated and compared for the validation.¹⁷

Lumbar FE Model Validation

The lumbar spine from LI-SI was validated by comparing the motion behavior of the FE model with the in vitro ROM data from Panjabi et al. ¹⁸ Panjabi et al. dissected the human cadaveric spine specimens from LI-SI; potted the SI vertebra. Io Nm moment was applied at LI to simulate flexion, extension, lateral bending, and axial rotation in their in vitro study. The same loading scenarios were simulated on the finite element model from LI pelvis for validation of the model. The pelvis was fixed, and the loads were applied at LI. The ROM of LI-SI was evaluated and compared for the validation. ¹⁸

Table 2. Follower Load on Each Vertebral Body Based on the Body Weight of 80.7 kg

Vertebral Body	%	Value
T1	14	80.7(Kg)*0.14*9.8 = 111
T2	16.6	131
T3	19.2	152
T4	21.8	172
T5	24.4	193
T6	27	214
T7	29.6	234
T8	32.2	255
Т9	34.8	275
T10	37.4	296
T11	40	316
T12	42.6	337
L1	45.2	357
L2	47.8	378
L3	50.4	399
L4	53	419
L5	55.6	440
S1	58.2	460

Development of Different Sagittal Alignment Models

The spinopelvic parameters such as SVA, LL, TK, PI, PT, and SS were modified iteratively by applying loads in the sagittal plane to develop 3 different sagittal alignment models, simulating the Schwab adult spinal deformity classification and different compensatory-mechanisms.^{8,12} As shown in Figure 2, these were (1) Balanced/Normal (SVA = 0 mm, LL = 50° , TK = 25° , PI = 45° , PT = 10° , SS = 35°), validated baseline model described earlier; (2) Balanced with compensatory mechanisms/Flat back $(SVA = 50 \text{ mm}, LL = 20^{\circ}, TK = 20^{\circ}, PI = 45^{\circ}, PT = 30^{\circ}, SS =$ 15°); and (3) Imbalanced/Hyperkyphotic (HK) (SVA = 150 mm, $LL = -5^{\circ}$, $TK = 25^{\circ}$, $PI = 45^{\circ}$, $PT = 40^{\circ}$, $SS = 5^{\circ}$). The compensatory mechanism was simulated by decreasing TK and pelvic retroversion. The HK model represented an imbalanced model in which the sagittal balance deteriorated due to the lack of a compensation mechanism. Hip joints of all the models simulated the standing posture and the distal femurs were fixed. The follower load technique was used to simulate the load at different vertebral levels due to upper body mass and muscle contractions as described by Schultz et al. 19-22 The loads were applied from T1 to S1 levels as a percentage of the body weight of a 55-year-old healthy North American male (80.7 kg) (Table 2).²³ Pure moments of 2 Nm and 5.5 Nm (total 7.5 Nm) were applied at T1 and L1, respectively, to simulate flexion, extension, left/ right bending, and left/right axial rotation. 17,24 The maximum nodal von Mises stress values in the cortical portion of vertebral bodies, annulus fibrosus, and nucleus pulposus (intradiscal

pressure [IDP]) were calculated twice: after applying follower load and follower load + pure moment.

Data Analysis

The stresses of the normal, flat back and hyper-kyphotic alignments were obtained by using the mean of the segmental stress values of maximum cortical vertebral stress, annular stresses and intra discal pressures (IDP). The percentage changes for the recorded cortical vertebral stress, annular stress and IDP for the flat back and HK model at each segment were calculated with respect to the normal model and compared to the different sagittal alignments.

Percentage change of flat back (F) or HK models with respect to normal (N) model were calculated as follows:

Percentage change (%) =
$$\frac{(F \text{ or } HK - N)}{N} \star_{100}$$

RESULTS

Model Validation

Thoracic FE Model Validation. All predicted ROMs were within the experimental range (Watkins et al.): flexion-extension 14° (experimental range: $3.11^{\circ}-29.29^{\circ}$), left/right lateral bending 9.18° (experimental range: $3.71^{\circ}-27.96^{\circ}$), and left/right axial rotations 34.6° (experimental range: $11.95^{\circ}-67.55^{\circ}$). 17

Lumbar FE Model Validation. All predicted ROMs were within the experimental ROM (Panjabi et al.): flexion-extension 35.8° (experimental range: $25.2^{\circ}-76^{\circ}$), left/right lateral bending 21° (experimental range: $20^{\circ}-67^{\circ}$), and left/right axial rotations 17.4° (experimental range: $2.75^{\circ}-21.6^{\circ}$). ¹⁸

Stress Analyses

Maximum Cortical Vertebral Stress (MPa). The cortical vertebral stresses for the HK model were higher for all the motions compared with normal and flat back models (Figure 3), when only the follower load was applied to the models. The stresses in the HK model increased by 86% compared with the normal model while the stresses for flat back model decreased by 3% compared with the normal model. When bending motions were applied along with the follower loads, the overall stresses for the HK model increased by 4%, 25%, 21%, 20%, 26%, and 23% compared with the normal model for extension, flexion, left bending, right bending, left rotation, and right rotation, respectively. Also, the stresses in the flat back model increased by 5% for flexion and showed a decrease of 2%, 3%, 1%, 9%, and 4% compared to normal model for extension, left bending, right bending, left rotation, and rotation, respectively.

The maximum change in stresses was seen for flexion motion, therefore the stress values observed at each level of the thoracolumbar spine were further analyzed to compare the 3 alignments. In particular, the stresses for the HK model increased by 40%, 54%, and 30% at T10, T11, and T12 compared with the normal model, respectively. However, the stresses at these levels for the flat back model were similar to the normal model.

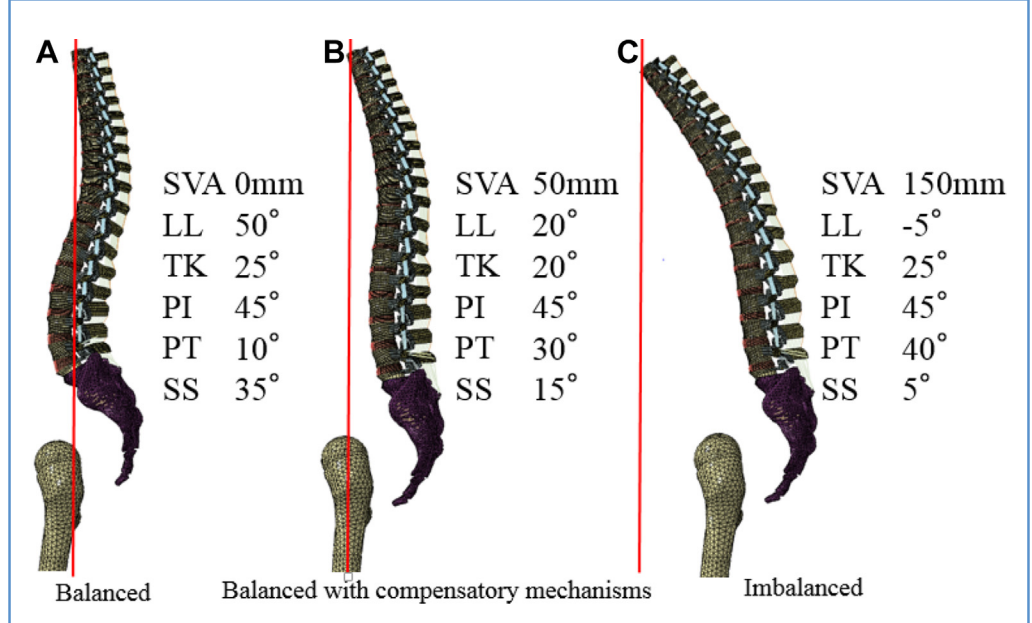
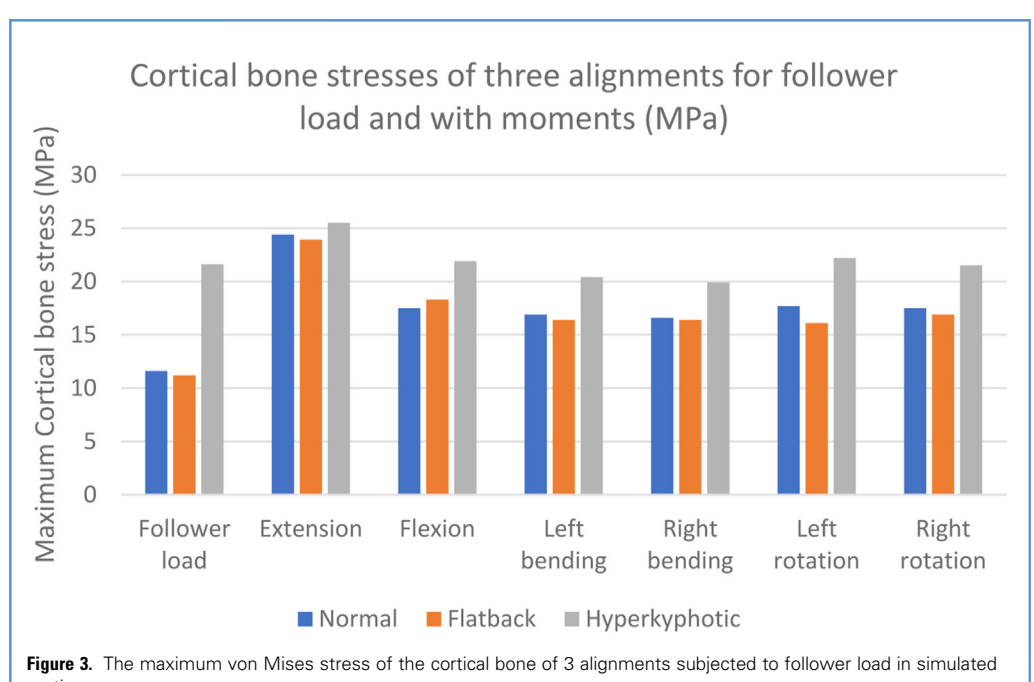
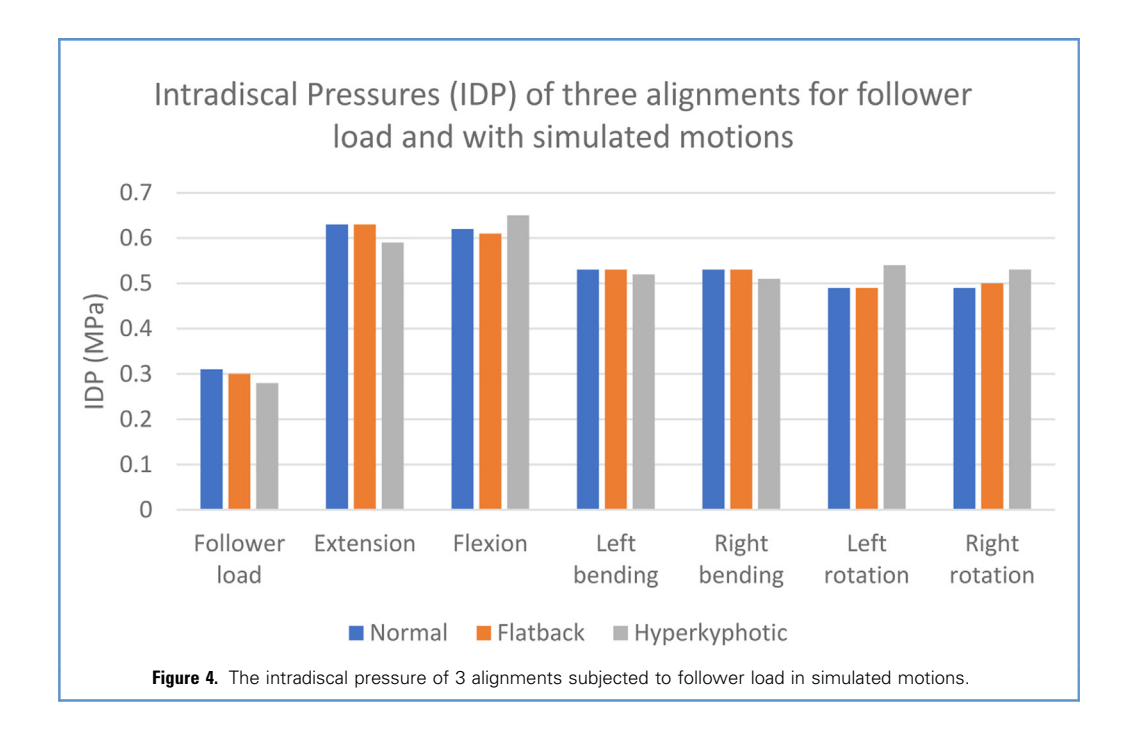


Figure 2. Three different finite element models used to investigate the biomechanics of different sagittal alignments. Red line indicates the C7 plumb line

Maximum Intradiscal Pressure (IDP). The IDP for the HK model decreased by 8% compared with the normal model (Figure 4) when only the follower load was applied. The IDP increased by 5%, 8%, and 7% for flexion, left rotation, and right rotation,

respectively, and decreased by 6%, 2%, 5% for extension, left bending, and right bending, respectively, compared with the normal model when the follower load and the bending motions were applied. The flat back model showed a decrease in IDP of





less than 2% when compared with the normal model for the follower load only and follower load plus bending motion loading scenarios.

The maximum change in IDP was seen for flexion motion, therefore the IDPs at each level of the thoracolumbar spine for flexion was analyzed to compare the 3 alignments. The IDP for the HK model increased at T10-T11, L1-L2, and L2-L3 by 7%, 30%, and 18%, while decreased by 2% and 8% at T11-T12 and T12-L1 compared with the normal model, respectively. The flat back model showed an increase of 12% at L1-L2 and decreased by less than 1% for the other thoracolumbar spinal levels compared with the normal model.

Maximum Annular Stress (MPa). The overall annular stresses for the HK model showed an increase of 19% for the follower load only scenario compared with the normal model (Figure 5). The stresses increased by 48%, 22%, 14%, 34%, and 27% for flexion, left bending, right bending, left rotation, and right rotation for the HK model and decreased by 6% in extension compared with the normal model, respectively. The stresses increased by 2% for flexion for the flat back model and decreased by 21%, 21%, 13%, 11%, and 13% for extension, left bending, right bending, left rotation, and right rotation compared with the normal model, respectively.

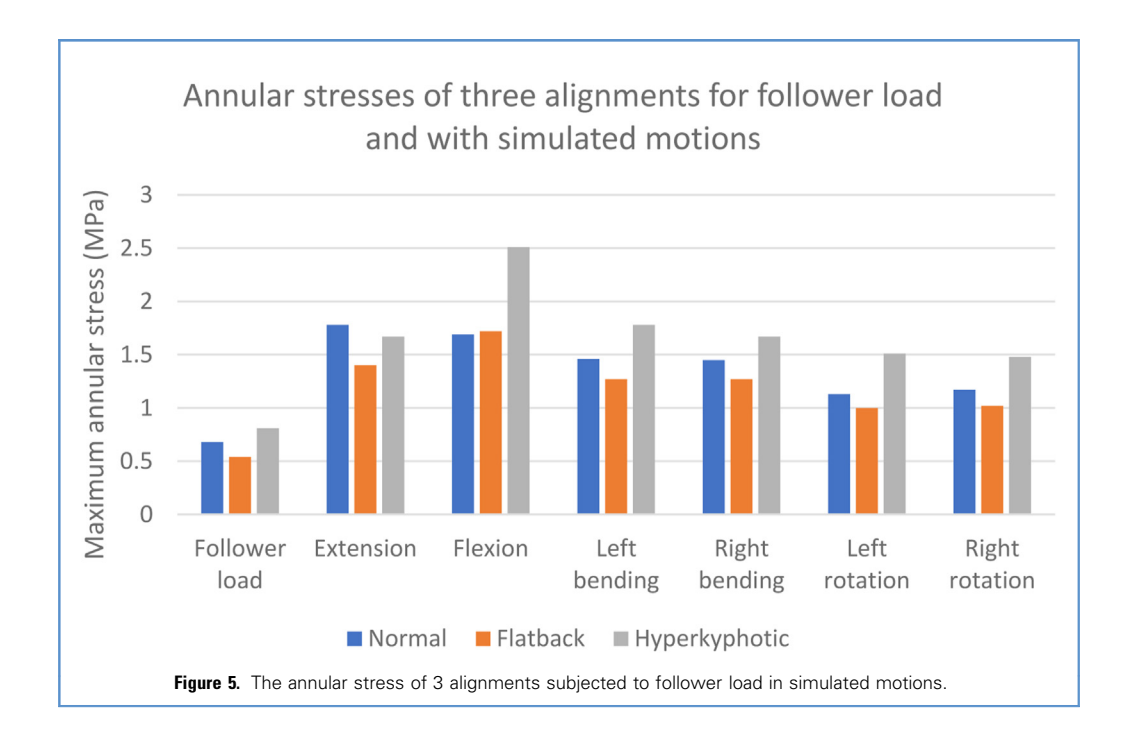
The maximum change in annular stress was seen for the flexion motion, therefore the annular stresses recorded at each level of the thoracolumbar spine for flexion were used to compare the 3 alignments. For the HK model, the annular stress increased at T10-T11, T12-L1, and L1-L2 increased by 38%, 92%, and 18%, and showed 11% decrease at T11-T12 compared with the normal model. The flat back model showed an increase of 6% at T12-L1, and a decrease of 31% at L1-L2 compared with the normal model.

The thoracolumbar region stress contours comparison for the flexion motion showing the maximum effect as a function of sagittal balance are shown in Figures 6 and 7. The higher stresses are seen for the HK model compared with the flat back and normal models at the thoracolumbar regions (Figure 6). The sagittal stress contours (Figure 7) show the higher stresses at the anterior and the middle regions of the vertebral bodies for the HK model compared with the flat back and normal models.

DISCUSSION

Recently, the sagittal balance has become crucial for clinical studies to understand adult spinal deformities. It has become evident that good clinical outcomes in spinal deformity treatment require proper alignment restoration. To minimize energy expenditure, SVA should be restored.11 Understanding whole spinal alignment and the dynamics of spinopelvic alignment is essential to restore sagittal balance while minimizing the risk of sagittal decompensation after surgical intervention.²⁵ Before these aspects can be explored, there is a need to understand segmental spinal stresses for normal and imbalanced spinal alignments for a possible treatment plan of a patient with spinal deformity as it would require integration of the pelvis in the preoperative evaluation and the treatment plan. 15 According to Rothenfluh et al., patients with sagittal imbalance exhibit a 10times higher risk for undergoing revision surgery if the sagittal balance is not maintained after the lumbar fusion surgery.²⁰

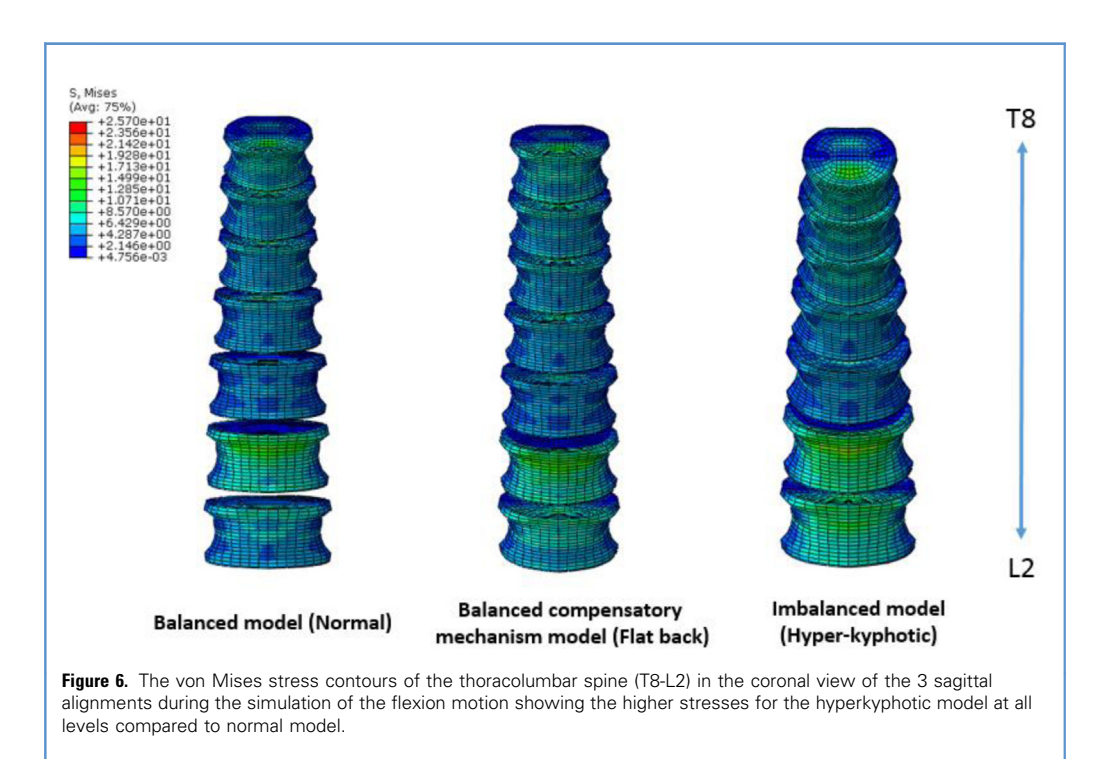
Galbusera et al. and Liu et al. conducted a finite element study of a lumbar spine for standing and inflexed posture, and both studies showed that an increase in the lumbar loads led to an increase in spinal lordosis. However, no reports have investigated the change in stress distribution across the spinal



column in ASD. To study the biomechanics of adult spine deformity, we created the balanced model (Normal), the balanced compensatory mechanism model (Flatback), and the imbalanced model (HK) with reference to Schwab's classification.^{8,12} The results showed that the stresses increased

on the spine with the deterioration of the sagittal balance from normal model to flat back (with compensatory mechanism) and imbalanced HK model.

The results for a person standing with only follower load applied indicated that stresses at the flat back model were similar



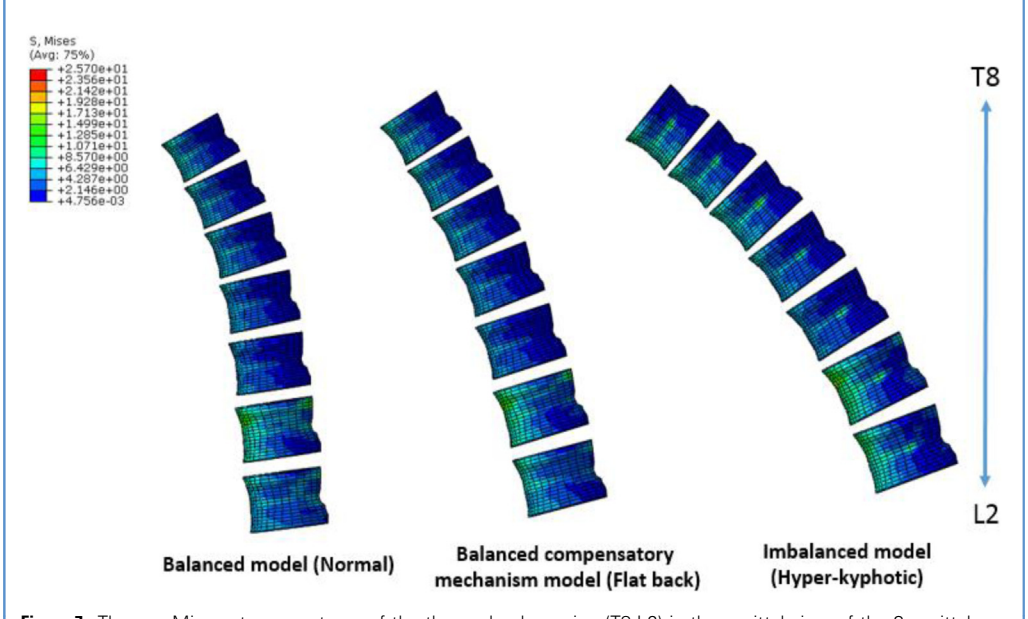


Figure 7. The von Mises stress contours of the thoracolumbar spine (T8-L2) in the sagittal view of the 3 sagittal alignments during the simulation of the flexion motion showing the higher stresses for the hyperkyphotic model at all the levels compared to normal model.

to the normal model, but for the HK model, the stresses were higher for the vertebrae. The stresses at the annulus and IDP showed a similar trend for the normal, flat back, and HK models. The maximum impact on overall stresses as a function of sagittal imbalance was observed for the flexion motion at all the spinal segments. This shows that the sagittal imbalance affects overall stresses on the spine due to the posture. The results for the follower load along with the motion showed that the increase in the stresses on the HK model was higher compared with the flat back model.

The deterioration of sagittal balance may be involved in osteoporotic vertebral fractures and low back pain.²⁹ The deterioration of the sagittal balance had the greatest influence on the thoracolumbar junction. Osteoporotic vertebral fractures are more prevalent at the thoracolumbar junction, and about half occur without obvious trauma.30 Significant relationships were found between sagittal spinopelvic parameters in osteoporotic patients of older age.²⁹ An abnormal kyphotic posture is considered a result of osteoporotic vertebral fractures represented with an anterior wedge deformity, which is a cause of local kyphosis in the elderly population.³¹ Our results indicate that deterioration of sagittal balance due to aging (represented by the HK model) may be one of the causes of atraumatic vertebral fractures with the possibility of the bone fracture occurring at the thoracolumbar junction, as shown by the stress contours (Figures 6 and 7). The vertebral body fractures cause kyphosis leading to lower health-related QOL.32-34

Several studies have found a correlation between thoracolumbar and spinopelvic sagittal parameters and degenerative disc disease (DDD). Liu et al. conducted a retrospective analysis on MRI images obtained from adult patients with DDD.³⁵ They observed a significant correlation between sagittal parameters and the incidence of DDD at the thoracolumbar junction and lumbosacral junction. They observed that high thoracolumbar kyphosis was associated with the prevalence of DDD and contributed significantly to the progression of DDD at the thoracolumbar junction. The incidence of DDD at the lumbosacral junction had a statistically significant correlation with PI. Patients with a high PI had a predisposition towards DDD at the lumbosacral junction. Similar observations were found by the retrospective magnetic resonance imaging (MRI) study conducted by Keorochana et al.³⁶ Their group found a significant correlation in the frequent incidence of DDD at the thoracolumbar and lumbosacral junction and patients with high kyphosis.

Farshad-Amacker et al. observed in their retrospective MRI analysis study that maintenance of LL had a protective effect on the incidence rate as well as the progression of lumbar DDD.³⁷ Egrun et al. conducted a retrospective study on young female patients showing that a decrease in LL had a statistically significant effect on the progression/incidence of DDD as well as the incidence of disc herniation.³⁸ Adams et al. found that degenerative disc disease shifts the compressive load-bearing capacity of the vertebral body posteriorly, reducing the trabecular bone network in the anterior aspect of the vertebra.³⁹ This may predispose patients with degenerative disc disease to anterior vertebral fractures.

The negative cascade seen in our study suggests that sagittal imbalance induces a vertebral body fracture, which leads to another vertebral fracture causing a severe sagittal imbalance, which may drastically reduce patient QOL. To prevent this cascade, it may be necessary to prevent the deterioration of the sagittal balance by a proper treatment plan. The most crucial finding of this study is that the influence of deterioration in sagittal balance on the spinal stresses is expressed using numerical values. The limitations of this study include the absence of the ribcage and coronal deformities in the FE models. Nishida et al. used the finite element method to study the effects of the presence or absence of a rib cage on the spine. 40 They reported that the model with a rib cage suppressed the strain in the middle thoracic spine compared to the model without it. Therefore, they concluded that a rib cage increased the stability of the thoracic spine. Because the rib cage has a great impact on the spine, further study will be necessary using model with a rib cage.40 Additionally, the FE model used in the current study lacks the musculature surrounding the spine and does not take the potential effects of these musculoskeletal forces into account.

CONCLUSIONS

The spinal column stresses increase with the increasing level of sagittal imbalance. When the sagittal balance breaks down, the

overall spinal stresses worsen, especially at the thoracolumbar junction. Degradation of sagittal balance leads to an increase in stresses near the thoracolumbar junction that may lead to atraumatic anterior fractures and disc degeneration.

CREDIT AUTHORSHIP CONTRIBUTION STATEMENT

Koji Matsumoto: Read and approved the final submitted manuscript, Methodology, Writing — review & editing, FE models, Acquisition for results, Writing — original draft. Anoli Shah: Read and approved the final submitted manuscript, FE models, Acquisition for results, Writing — original draft. Amey Kelkar: Read and approved the final submitted manuscript, FE models, Acquisition for results, Writing — original draft. Muzammil Mumtaz: Read and approved the final submitted manuscript, Data acquisition, Writing — review & editing. Yogesh Kumaran: Read and approved the final submitted manuscript, Data acquisition, Writing — review & editing. Vijay K. Goel: Read and approved the final submitted manuscript, Writing — review & editing, Primary investigator, Guide for the study.

REFERENCES

- I. Sieh KM, Chan YY, Ho PY, Fung KY. What is the best lateral radiograph positioning technique for assessment of sagittal balance: a biomechanical study on influence of different arm positions. J Orthop Surg. 2018;26: 2309499018770932.
- Glassman SD, Berven S, Bridwell K, Horton W, Dimar J. Correlation of radiographic parameters and clinical symptoms in adult scoliosis. Spine. 2005;30:682-688.
- Schwab F, Patel A, Ungar B, Farcy JP, Lafage V. Adult spinal deformity—postoperative standing imbalance: how much can you tolerate? An overview of key parameters in assessing alignment and planning corrective surgery. Spine. 2010;35: 2224-2231.
- Roussouly P, Nnadi C. Sagittal plane deformity: an overview of interpretation and management. Eur Spine J. 2010;19:1824-1836.
- Glassman SD, Bridwell K, Dimar JR, Horton W, Berven S, Schwab F. The impact of positive sagittal balance in adult spinal deformity. Spine. 2005;30:2024-2029.
- Rose PS, Bridwell KH, Lenke LG, et al. Role of pelvic incidence, thoracic kyphosis, and patient factors on sagittal plane correction following pedicle subtraction osteotomy. Spine. 2009;34: 785-791.
- Lee CS, Chung SS, Kang KC, Park SJ, Shin SK. Normal patterns of sagittal alignment of the spine in young adults radiological analysis in a Korean population. Spine. 2011;36:E1648-E1654.
- 8. Schwab F, Ungar B, Blondel B, et al. Scoliosis Research Society—Schwab adult spinal deformity

- classification: a validation study. Spine. 2012;37: 1077-1082.
- Schwab FJ, Blondel B, Bess S, et al. Radiographical spinopelvic parameters and disability in the setting of adult spinal deformity: a prospective multicenter analysis. Spine. 2012;38:E803-E812.
- Ames CP, Smith JS, Scheer JK, et al. Impact of spinopelvic alignment on decision making in deformity surgery in adults: a review. J Neurosurg Spine. 2012;16:547-564.
- Shah AA, Lemans JV, Zavatsky J, et al. Spinal balance/alignment—clinical relevance and biomechanics. J Biomed Eng. 2019;141. https:// doi.org/10.1115/1.4043650.
- Roussouly P, Pinheiro-Franco JL. Biomechanical analysis of the spino-pelvic organization and adaptation in pathology. Eur Spine J. 2011;20: 609-618.
- Jones AD. Biomechanical and Finite Element Analyses of Alternative Cements for Use in Vertebral Kyphoplasty [Dissertation.]. Toledo, OH: University of Toledo; 2013.
- Gerber JM. Biomechanical Evaluation of Facet Bone Dowels in the Lumbar Spine [Dissertation.]. Toledo, OH: University of Toledo; 2015.
- Schwab F, Lafage V, Patel A, Farcy JP. Sagittal plane considerations and the pelvis in the adult patient. Spine. 2009;34:1828-1833.
- Palepu V. Biomechanical Effects of Initial Occupant Seated Posture due to Rear End Impact Injury [Dissertation.]. Toledo, OH: University of Toledo; 2013.
- Watkins R IV, Watkins R III, Williams L, et al. Stability provided by the sternum and rib cage in the thoracic spine. Spine. 2005;30:1283-1286.

- Panjabi MM, Oxland TR, Yamamoto I, Crisco JJ. Mechanical behavior of the human lumbar and lumbosacral spine as shown by three-dimensional load-displacement curves. J Bone Jt Surg Am. 1994; 76:413-424.
- Schultz A, Andersson GB, Ortengren R, Björk R, Nordin M. Analysis and quantitative myoelectric measurements of loads on the lumbar spine when holding weights in standing postures. Spine. 1982: 300-307.
- Agarwal A, Agarwal AK, Jayaswal A, Goel V. Smaller interval distractions may reduce chances of growth rod breakage without impeding desired spinal growth: a finite element study. Spine Deform. 2014;2:430-436.
- 21. Agarwal A, Agarwal AK, Jayaswal A, Goel V. Effect of distraction force on growth and biomechanics of the spine: a finite element study on normal juvenile spine with dual growth rod instrumentation. Spine Deform. 2014;2:260-269.
- 22. Patwardhan AG, Havey RM, Meade KP, Lee B, Dunlap B. A follower load increases the load-carrying capacity of the lumbar spine in compression. Spine. 1999;24:1003-1009.
- Walpole SC, Prieto-Merino D, Edwards P, et al. The weight of nations: an estimation of adult human biomass. BMC Pub Health. 2012;12:1-6.
- 24. Dreischarf M, Zander T, Bergmann G, Rohlmann A. A non-optimized follower load path may cause considerable intervertebral rotations.

 J Biomech. 2010;43:2625-2628.
- Makhni MC, Shillingford JN, Laratta JL, Hyun SJ, Kim YJ. Restoration of sagittal balance in spinal deformity surgery. J Korean Neurosurg Soc. 2018;61: 167

- Rothenfluh DA, Mueller DA, Rothenfluh E, Min K. Pelvic incidence-lumbar lordosis mismatch predisposes to adjacent segment disease after lumbar spinal fusion. Eur Spine J. 2015; 24:1251-1258.
- 27. Galbusera F, Brayda-Bruno M, Costa F, Wilke HJ. Numerical evaluation of the correlation between the normal variation in the sagittal alignment of the lumbar spine and the spinal loads. J Orthop Res. 2014;32:537-544.
- 28. Liu T, Khalaf K, Naserkhaki S, El-Rich M. Loadsharing in the lumbosacral spine in neutral standing & flexed postures—a combined finite element and inverse static study. J Biomech. 2018; 70:43-50.
- Lee JS, Lee HS, Shin JK, Goh TS, Son SM. Prediction of sagittal balance in patients with osteoporosis using spinopelvic parameters. Eur Spine J. 2013;22:1053-1058.
- 30. Tsujio T, Nakamura H, Terai H, et al. Characteristic radiographic or magnetic resonance images of fresh osteoporotic vertebral fractures predicting potential risk for nonunion: a prospective multicenter study. Spine. 2011;36:1229-1235.
- Burger H, Van Daele PL, Grashuis K, et al. Vertebral deformities and functional impairment in men and women. J Bone Miner Res. 1997;12: 152-157.

- Lyles KW, Gold DT, Shipp KM, Pieper CF, Martinez S, Mulhausen PL. Association of osteoporotic vertebral compression fractures with impaired functional status. Am J Med. 1993;94: 595-601.
- Pluijm SM, Tromp AM, Smit JH, Deeg DJ, Lips P. Consequences of vertebral deformities in older men and women. J Bone Miner Res. 2000;15: 1564-1572.
- 34. Ensrud KE, Thompson DE, Cauley JA, et al. Prevalent vertebral deformities predict mortality and hospitalization in older women with low bone mass. J Am Geriatr Soc. 2000;48:24I-249.
- 35. Liu H, Shrivastava SR, Zheng ZM, et al. Correlation of lumbar disc degeneration and spinal-pelvic sagittal balance. Zhonghua yi xue za zhi. 2013;93: 1123-1128.
- Keorochana G, Taghavi CE, Lee KB, et al. Effect of sagittal alignment on kinematic changes and degree of disc degeneration in the lumbar spine: an analysis using positional MRI. Spine. 2011;36: 893-898.
- Farshad-Amacker NA, Hughes AP, Aichmair A, Herzog RJ, Farshad M. Determinants of evolution of endplate and disc degeneration in the lumbar spine: a multifactorial perspective. Eur Spine J. 2014;23:1862-1868.

- Ergun T, Lakadamyali H, Sahin M. The relation between sagittal morphology of the lumbosacral spine and the degree of lumbar intervertebral disc degeneration. Acta Orthop Traumatol Turc. 2010;44: 293-299.
- Adams MA, Pollintine P, Tobias JH, Wakley GK, Dolan P. Intervertebral disc degeneration can predispose to anterior vertebral fractures in the thoracolumbar spine. J Bone Miner Res. 2006;21:1409-1416.
- 40. Nishida N, Ohgi J, Jiang F, et al. Finite element method analysis of compression fractures on whole-spine models including the rib cage. Comput Math Methods Med. 2019;4:1-10.

Conflict of interest statement: The work was supported in part by NSF Industry/University Cooperative Research Center at The University of California at San Francisco, San Francisco, CA, The University of Toledo, Toledo, OH, and The Ohio State University, Columbus, OH (www.nsfcdmi.org).

Received 11 June 2022; accepted 25 August 2022

Citation: World Neurosurg. (2022) 167:e962-e971. https://doi.org/10.1016/j.wneu.2022.08.119

Journal homepage: www.journals.elsevier.com/world-neurosurgery

Available online: www.sciencedirect.com

1878-8750/\$ - see front matter © 2022 Elsevier Inc. All rights reserved.